

## **<sup>29</sup>Si NMR and Small-Angle X-ray Scattering Studies of the Effect of Alkaline Ions (Li<sup>+</sup>, Na<sup>+</sup>, and K<sup>+</sup>) in Silico-Alkaline Sols**

**Fabien Gaboriaud,\* André Nonat, and Denis Chaumont**

*Laboratoire de Recherches sur la Réactivité des Solides (UMR 5613), Université de Bourgogne, 9 av Alain Savary, BP47870-21078 Dijon Cedex, France*

**Aldo Craievich**

*Laboratorio Nacional de Luz Sincrotron/CNPq, Campinas, SP, Brazil and Instituto de Física/USP, Sao Paulo, Brazil*

**Bernard Hanquet**

*Laboratoire de Synthèse et d'Electrosynthèse Organométalliques (UMR 5632), Université de Bourgogne, bd Gabriel 21000 Dijon, France*

*Received: October 14, 1998*

Alkali–silica reactions (ASR) which occur in concrete can be simulated in laboratory by destabilization of silico-alkaline aqueous solutions by addition of calcium ions. The relevant features of the reaction depend on the nature of alkaline ions (Li<sup>+</sup>, Na<sup>+</sup>, or K<sup>+</sup>) and on the silica/alkaline ratios which fix the distribution of the molecular species in the precursor solution. <sup>29</sup>Si NMR spectroscopy and small-angle X-ray scattering (SAXS) techniques were used to study the structure and size distribution of molecular and colloidal species in sols with different silica/alkaline molar ratio and several types of alkaline ions. Experimental SAXS curves were simulated using a simple structural model which assumes the sol to be composed of a multimodal set of weakly interacting hard spheres immersed in a liquid matrix. The results indicate the existence of strong interactions between alkaline ion and hydroxide and between alkaline ion and silicate species. The formation of large species (cyclic molecules and colloidal particles) is enhanced in solutions containing lithium. These results are consistent with those of previous investigations.

### **I. Introduction and Basic Aspects of Alkali–Silica Reaction**

Concrete is a porous material constituted of aggregates immobilized in a cement paste. Inter- and intra-aggregate pores are filled with a very basic aqueous solution which contains silicate, calcium, sodium, potassium, and hydroxide ions. Alkali–silica reaction (ASR) is a pathogenic reaction occurring in concrete which often leads to cracking effects. It is the consequence of interactions between the pore solution and reactive silica contained in some aggregates. The product is a calcium–alkaline–silica gel.

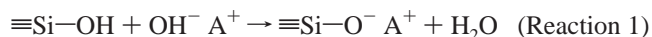
The initial stage of ASR is the attack of aggregates by the aqueous solution, mainly by hydroxide ions, which leads to the degradation of reactive silica. This degradation induces the formation of more or less polymerized silicate species in solution and the ionization of residual silica. The product (calcium–alkaline–silica gel) results from the reaction between the alkali silicate species in solution and the calcium ions provided by the cement paste.

However, the mechanism responsible for the expansion and cracking of concrete is still unclear. One of the critical parameters involved in this effect is the reactive silica content. It has been established, by measuring the expansion of concrete bars immersed in alkali hydroxide solutions, that the expansion coefficient exhibits a maximum when measured as a function of the reactive silica content in the aggregates.<sup>1</sup> The reactive silica content corresponding to maximum expansion is called

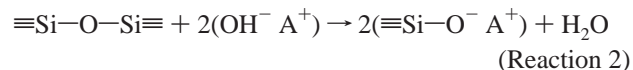
the “pessimum” content. On the other hand, expansion of concrete bars also depends on the nature of the alkaline cation. The addition of lithium compounds reduces the expansion of the concrete bars.<sup>2</sup>

The existence of a pessimum silica concentration has been correlated with the evolution of silica concentration in the solution when reactive silica is increasingly added into an alkali hydroxide solution<sup>3</sup> (Figure 1).

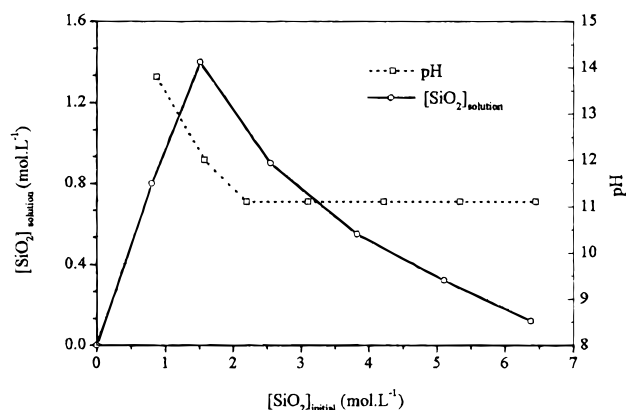
Two reactions occur together when alkaline hydroxide is mixed with reactive silica: (1) Ionization of silica surface (with A = Li, Na, K, or H):



(2) Dissolution of silica by breaking siloxane bonds:



These two reactions explain the decrease of the pH during the formation of the solutions. When thermodynamic equilibrium is reached, final conditions (pH, dissolved silica) are fixed by the amount of undissolved residual silica. If the initial solid silica content is low, silica dissolution is completed before the dissolution path reaches the solubility curve, meaning that the resultant solutions do not contain residual solid silica. On the other hand, if initial solid silica content is high, residual silica



**Figure 1.** Variation of silica concentration in solution and pH when reactive silica is increasingly added into an alkali hydroxide solution with a concentration of  $0.35 \text{ mol}\cdot\text{L}^{-1}$ .

removes hydroxide from solution by ionization of its surface (reaction 1) and the dissolution path reaches the limit at lower pH and therefore at lower silica concentration. Thus, at constant alkaline hydroxide concentration, the final quantity of silica passes through a maximum and then decreases, as the amount of initial solid silica in suspension increases.

The silicate solution, the residual ionized reactive silica and the calco-silico-alkaline gel formed from calcium ions and polysilicate solution, may be involved in the generation of the stresses which lead to cracking; the first two through a direct osmotic process<sup>4</sup> and the last one as a consequence of the crystallization pressure<sup>5</sup> or swelling<sup>6</sup> also induced by the osmotic process.

To examine the above-mentioned macroscopic properties, ASR is simulated in the laboratory using similar but simpler materials. The reaction is composed of two different stages:<sup>7–9</sup> (1) Dissolution of silica by hydroxide ions leading to the formation of a concentrated silico-alkaline aqueous solution, and (2) Destabilization of the alkaline silicate solution by the addition of calcium ions leading to the formation of a calcium alkaline silicate gel.

The properties of the products of the destabilization of alkaline solutions, by addition of Ca ions, strongly depend on the nature of the precursor sols. A notation usually employed for describing the composition of the precursor silico-alkaline solutions is the molar ratio between silica and the alkaline oxide ( $R_m = [\text{SiO}_2]/[\text{A}_2\text{O}]$  with A = alkaline). From a certain silica concentration, a gel is formed when solutions with silica/alkaline ratios,  $R_m$ , greater than 2 are destabilized. Conversely, when the solutions have a ratio less than 2 ( $R_m < 2$ ), a precipitate is formed.

On the other hand, Iler<sup>10</sup> and Dent Glasser<sup>11,12</sup> concluded from ultrafiltration studies that the increase in  $R_m$  enhances polymerization of silicate species. They also described the formation of colloidal particles (large species or entities with sizes between 10 and 1000 Å) occurring at molar ratio greater than 2. Harris et al.<sup>13</sup> confirmed these results by means of <sup>29</sup>Si NMR studies. All of these authors concluded that solutions with  $R_m < 2$ , which yield precipitates, are essentially constituted of monomeric species, whereas solutions ( $R_m > 2$ ) which yield a gel are essentially composed of octamers.

The effect of the nature of alkaline cation was studied by McCormick et al.<sup>14</sup> using alkali-metal cation NMR spectroscopy (<sup>23</sup>Na, <sup>39</sup>K, <sup>87</sup>Rb, <sup>133</sup>Cs). These authors established the presence of cation–anion pairs in alkaline silicate solutions and determined their concentration from the values of the chemical shifts and widths of the resonance lines. They concluded that the

concentration of ion pairs involving large anions increases with increasing cation size. This effect was not studied for lithium (<sup>7</sup>Li) because, in this case, the variation of chemical shift was too small to ensure reproducible results without the use of an internal standard.

Recent investigations<sup>15</sup> showed that the silico-calco-alkaline gel is mainly responsible for the development of stresses which are strong enough to produce the cracking of concrete. The characteristics of the formation and the properties of the gel for  $R_m > 2$  are highly dependent on the nature of the alkaline hydroxide in the silico-alkaline solution.<sup>9</sup> Gels formed by destabilization of lithium silicate solutions or potassium silicate solutions exhibit gelation times higher than those obtained from sodium silicate solutions at a constant calcium concentration. Calcium ions play an important role in this reaction because they bring together two silicate species and then leave the place to a siloxane bond.<sup>16</sup> These results indicate the presence of strong interactions between alkaline ion and silicate species. Therefore, these interactions prevent the formation of siloxane bond by calcium ion, especially in the case of lithium.

Silico-alkaline solutions have been studied using a number of techniques, namely trimethylsilylation,<sup>17</sup> ultrafiltration,<sup>10</sup> and light scattering.<sup>18</sup> The results indicate the existence of polysilicate ions, but they did not establish the structure of these silicate species. Harris et al.<sup>19,20</sup> and Enghelardt et al.<sup>21</sup> gave a structural description for a potassium silicate solution ( $[\text{K}_2\text{O}] = 0.75 \text{ M}$  and  $[\text{SiO}_2] = 1.5 \text{ M}$ ,  $R_m = 2$ ) enriched with the <sup>29</sup>Si isotope by using two-dimensional silicon-29 NMR correlation spectroscopy (COSY). They established the chemical shifts of each Si nucleus of 20 different silicate species. McCormick et al.<sup>22</sup> extended the structural assignments to sodium silicate solution. This was possible because similar structures were observed by trimethylsilylation on both potassium and sodium silicate solutions.

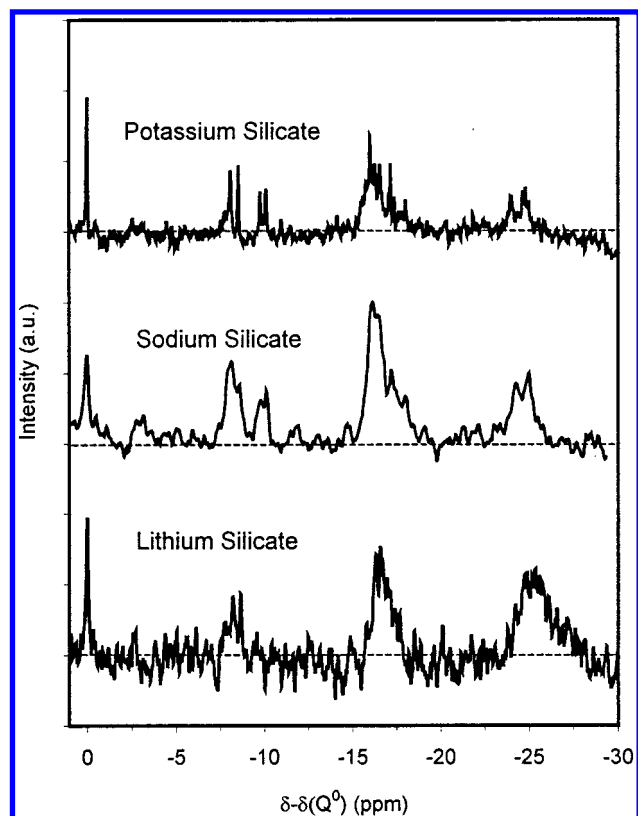
The knowledge of the precursor sols seems to be important in order to determine the characteristics of the gelation and the properties of the resulting gel. However, until now, no systematic and quantitative determination of the nature and structure distribution of the different species has been established as a function of the nature and concentration (or  $R_m$ ) of the alkaline hydroxide.

The purpose of this study is to describe, as quantitatively as possible, the structure and size distribution of the silicate species present in silico-alkaline solutions containing different alkaline ions ( $\text{Li}^+$ ,  $\text{Na}^+$ , or  $\text{K}^+$ ).

## II. Sample Preparation and Experimental Techniques

The studied sols were prepared by mixing silica (silicagel, Merck Gel de silice 60, 70–230 mesh ASTM), alkaline ( $\text{Li}^+$ ,  $\text{Na}^+$ , or  $\text{K}^+$ ) oxide, and water until complete dissolution (no filtration). Two sets of three sols with silica/alkaline molar ratios  $R_m = [\text{SiO}_2]/[\text{A}_2\text{O}] = 2$  and 3 were prepared, each of them with A = Li, Na, and K. The silica concentration was kept constant for all samples at  $1.5 \text{ mol}\cdot\text{L}^{-1}$  close to the pessimum condition.

All of the <sup>29</sup>Si NMR spectra were recorded using a Bruker DRX500 spectrometer operating at 99.36 MHz. The liquid samples were put inside poly(tetrafluoroethylene) (PTFE) (4 mm o.d.) tubes vertically located inside a 5 mm o.d. glass tube. Heavy water (10%) was added to the samples to lock the spectrometer. A pulse width of 90° (10.8 μs) with a repetition time optimized at 90 sec was identified. Free induction decays (fids) were recorded over a sweep width of 20 kHz (~200 ppm) using a 32 K data storage system. A “blank” fid corresponding



**Figure 2.**  $^{29}\text{Si}$  NMR spectra of the aqueous silico-alkaline solutions with a molar ratio  $R_m = 2$ . Chemical shifts were referenced to the position of the monomeric species.

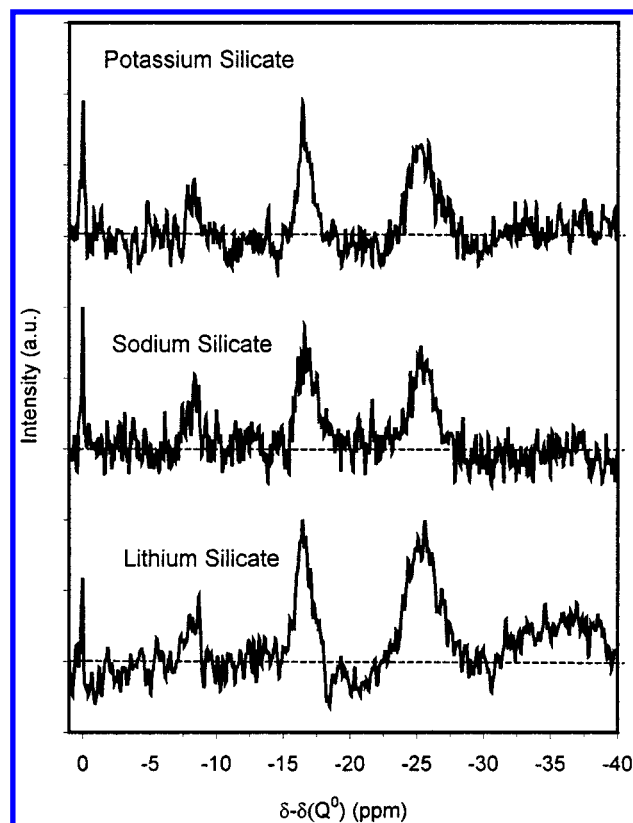
to the background of the probe inner tubes in  $\text{SiO}_2$  was subtracted from each data set. A line broadening was used to give a satisfactory signal-to-noise ratio. It was calculated by taking the full width at half maximum (fwhm) of the monomer's peak.

Silico-alkaline solutions were studied by single-angle X-ray scattering (SAXS) using the synchrotron radiation beamline D22, at LURE, Orsay, France. The X-ray beam was monochromatized using a bent single crystal which also focuses the beam in the horizontal plane at the detector position. The incident beam is defined by a set of slits. The scattered X-ray intensity  $I(q)$  was recorded, using a vertical 1D position sensitive detector, as a function of the modulus of the scattering vector,  $q$ , defined as  $q = (4\pi/\lambda)\sin(\theta/2)$ , where  $\lambda$  is the X-ray wavelength ( $\lambda = 1.609 \text{ \AA}$ ) and  $\theta$  is the scattering angle. The samples were placed inside a 1 mm thick cell with parallel thin kapton windows. The parasitic scattering produced by the collimating slits, Kapton windows, and air was subtracted from the total measured scattering intensity. Measurements were performed over a  $q$  domain ranging from  $10^{-2} \text{ \AA}^{-1}$  to  $0.8 \text{ \AA}^{-1}$ .

### III. Experimental Results

**A.  $^{29}\text{Si}$  NMR.** *A1. NMR Spectra.* The  $^{29}\text{Si}$  NMR spectra of the aqueous silico-alkaline solutions with molar ratios  $R_m = 2$  and 3 are plotted in Figures 2 and 3, respectively. Each peak corresponds to different silicon nucleus environment. The chemical shifts assigned to different molecular species by three different authors, for solutions with  $R_m = 2$ , are summarized in Table 1.

The connectivity of the Si nuclei in the silicate species are described by the usual  $Q^n$  notation.<sup>21</sup>  $Q$  represents a silicon nucleus connected to four oxygen forming a tetrahedron. The superscript  $n$  indicates the connectivity, i.e. the number of other




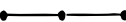


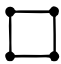
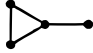


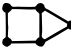





**Figure 3.**  $^{29}\text{Si}$  NMR spectra of the aqueous silico-alkaline solutions with a molar ratio  $R_m = 3$ . Chemical shifts were referenced to the position of the monomeric species.

$Q$  units attached to the  $\text{SiO}_4$  central tetrahedron. Thus,  $Q^0$  denotes the monomeric orthosilicate anion  $\text{SiO}_4^{4-}$ ,  $Q^1$  denotes end-groups of chains,  $Q^2$  denotes middle groups in chains or cycle,  $Q^3$  denotes chain branching sites, and  $Q^4$  denotes three dimensionally cross-linked groups. When the silicon nucleus is in a three-membered ring, the additional bond strain results in a downfield shift that creates two new chemical shift ranges designated by  $n = 2\Delta, 3\Delta$ . All peaks are referenced to the peak corresponding to monomeric silicate ( $Q^0$ ).

NMR spectra were simulated using Gaussian curves by adjusting the position, the intensity, and the fwhm. Because the fwhm of experimental peaks varies according to alkaline ion, it is kept constant at the monomer value. The values corresponding to the position of each Gaussian curve are given in Table 1. The simulated intensity obeying certain rules should fit to the experimental curve. The rules depend on the concentration of the species and on the number of silicon nuclei observed in these species. Most of species have more than one peak in the spectrum, each of them corresponds to one of the different silicon nuclei environments, i.e., species (3) or (7) or (12) (see Table 1). Therefore, the fitting of the spectrum must include the complete set of peaks of one species, keeping their peak integral ratios consistent with the number of silicon nuclei present in the species.

*A2. Determination of Species Fractions for Solutions with  $R_m = 2$ .* The simulation mentioned in the previous section was applied to the NMR spectra produced by the different silico-alkaline solutions with  $R_m = 2$ . An example of simulation corresponding to a silico-alkaline  $\text{SiO}_2/\text{K}_2\text{O} = 2$  is shown in Figure 4, which also includes the difference between the simulated and experimental spectra. These differences are of the order of the signal-to-noise ratio of the experiments. As an example, the peak positions corresponding to the species (7)

**TABLE 1: Reported  $^{29}\text{Si}$  Chemical Shifts, Referenced to the Peak Corresponding to Monomeric Silicate ( $\text{Q}^0$ ), for Different Silicate Species**

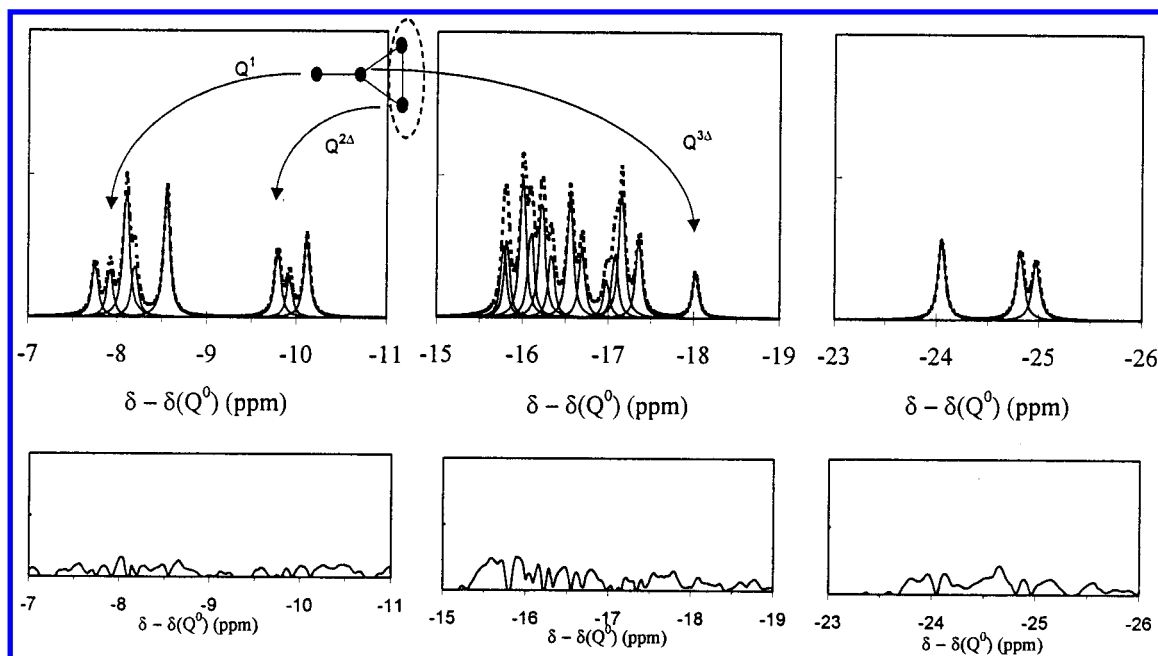
Oligomer <sup>d</sup>	Authors	$\text{Q}^1$	$\text{Q}^{2\Delta}$	$\text{Q}^2$	$\text{Q}^{3\Delta}$	$\text{Q}^3$
(2) dimer 	Engelhardt <i>et al.</i> <sup>a</sup>	-8.51				
	Harris <i>et al.</i> <sup>b</sup>	-8.59				
	McCormick <i>et al.</i> <sup>c</sup>	-8.1~8.3				
(3) linear trimer 	Engelhardt <i>et al.</i> <sup>a</sup>	-8.04		-16.92		
	Harris <i>et al.</i> <sup>b</sup>	-8.15		-16.7		
	McCormick <i>et al.</i> <sup>c</sup>	-8.1~8.3		-16.8~17.0		
(4) cyclic trimer 	Engelhardt <i>et al.</i> <sup>a</sup>		-10.13			
	Harris <i>et al.</i> <sup>b</sup>		-10.17			
	McCormick <i>et al.</i> <sup>c</sup>		-10.1~10.3			
(5) linear tetramer 	Engelhardt <i>et al.</i> <sup>a</sup>	-8.25		-16.17		
	Harris <i>et al.</i> <sup>b</sup>	-8.3		-16.4		
	McCormick <i>et al.</i> <sup>c</sup>	-8.1~8.3		-16.5~17.0		
(6) cyclic tetramer 	Engelhardt <i>et al.</i> <sup>a</sup>			-15.99		
	Harris <i>et al.</i> <sup>b</sup>			-16.09		
	McCormick <i>et al.</i> <sup>c</sup>			-16.2~16.5		
(7) branched cyclic trimer 	Engelhardt <i>et al.</i> <sup>a</sup>	-7.92	-9.78		-18.09	
	Harris <i>et al.</i> <sup>b</sup>	-8.06	-9.86		-18.22	
	McCormick <i>et al.</i> <sup>c</sup>	-8.1~8.3	-9.8~10.1		-18.2~18.4	
(8) bridged cyclic tetramer 	Engelhardt <i>et al.</i> <sup>a</sup>			-14.2		-21.94
	Harris <i>et al.</i> <sup>b</sup>			-14.22		-21.94
	McCormick <i>et al.</i> <sup>c</sup>			-14.2		-21.9
(9) monosubstituted cyclic tetramer 	Engelhardt <i>et al.</i> <sup>a</sup>	-7.86		-15.7, -16.0		-23.99
	Harris <i>et al.</i> <sup>b</sup>	-7.9		-15.84		-24.2
	McCormick <i>et al.</i> <sup>c</sup>	none		none		none
(10) bicyclic pentamer 	Engelhardt <i>et al.</i> <sup>a</sup>		-9.86	-16.28	-17.11	
	Harris <i>et al.</i> <sup>b</sup>		-9.86	-16.3	-17.16	
	McCormick <i>et al.</i> <sup>c</sup>		-9.9~10.0	-16.4	-17	
(11) prismatic hexamer 	Engelhardt <i>et al.</i> <sup>a</sup>				-17.08	
	Harris <i>et al.</i> <sup>b</sup>				-17.22	
	McCormick <i>et al.</i> <sup>c</sup>				-17.2	
(12) tricyclic hexamer 	Engelhardt <i>et al.</i> <sup>a</sup>			-16.12	-16.6, -17.5	-24.74
	Harris <i>et al.</i> <sup>b</sup>			-16	-16.6, -17.4	-24.72
	McCormick <i>et al.</i> <sup>c</sup>			-16.1	-16.7, -17.3	-24.7
(13) cubic octamer 	Engelhardt <i>et al.</i> <sup>a</sup>					-27.31
	Harris <i>et al.</i> <sup>b</sup>					none
	McCormick <i>et al.</i> <sup>c</sup>					-27.2~27.5
(14) tricyclic octamer 	Engelhardt <i>et al.</i> <sup>a</sup>					none
	Harris <i>et al.</i> <sup>b</sup>					none
	McCormick <i>et al.</i> <sup>c</sup>					-24.7
(15) tetracyclic nonamer 	Engelhardt <i>et al.</i> <sup>a</sup>					none
	Harris <i>et al.</i> <sup>b</sup>					none
	McCormick <i>et al.</i> <sup>c</sup>					-25

<sup>a</sup> Reference 21. <sup>b</sup> References 19 and 20. <sup>c</sup> Reference 22. <sup>d</sup> Silicon atoms are marked by a black dot, oxygen atoms are omitted. Q represents a silicon nucleus connected to four oxygen forming a tetrahedron. The superscript  $n$  indicates the connectivity of this nucleus. When the Si nucleus is in a three-membered ring,  $n$  is noted  $2\Delta$  or  $3\Delta$ .

are indicated. By integrating the Gaussian curves, the fractions of the number of silicate species present are obtained. The results corresponding to solutions with  $\text{SiO}_2/\text{Li}_2\text{O}$ ,  $\text{SiO}_2/\text{Na}_2\text{O}$ , and  $\text{SiO}_2/\text{K}_2\text{O}$  solutions for  $R_m = 2$  are presented in Table 2.

**A3. NMR Results Corresponding to Sols with  $R_m = 3$ .** In the  $^{29}\text{Si}$  NMR spectra corresponding to samples with a silica/alkaline molar ratio  $R_m = 3$  (Figure 3), another group of peaks appears between  $-30$  and  $-40$  ppm. Harris *et al.*<sup>13</sup> assigned these peaks





**Figure 4.** Simulation (top) and difference (bottom) of the experimental spectrum for silico-alkaline solution with potassium with a molar ratio  $R_m = 2$ . An example of assignments is shown for species 7 (branched cyclic trimer).

**TABLE 2: Distributions of Silicate Species in Number Percent Determined from  $^{29}\text{Si}$  NMR Experiments for Three Studied Silico-Alkaline Solutions with Silica/Alkaline Molar Ratios  $R_m = 2$**

% oligomer	$R_m = 2$		
	$\text{SiO}_2\text{--Li}_2\text{O}$	$\text{SiO}_2\text{--Na}_2\text{O}$	$\text{SiO}_2\text{--K}_2\text{O}$
(1) monomer	34.2	28.3	33.7
(2) dimer	7.2	8.0	8.9
(3) linear trimer	5.0	10.2	4.3
(4) cyclic trimer	0	5.6	3.7
(5) linear tetramer	7.3	11.1	8.9
(6) cyclic tetramer	5.3	7.7	4.3
(7) branched cyclic trimer	6.1	1.6	5.6
(9) monosubstituted cyclic tetramer	4.8	5.4	12.6
(10) bicyclic pentamer	7.3	9.5	4.8
(11) prismatic hexamer	0	3.3	3.0
(12) tricyclic hexamer	8.0	4.9	9.3
(14) tricyclic octamer	2.1	1.5	0
(15) tetracyclic nonamer	12.7	2.9	0.9

to  $Q^4$  environments which form the core of relatively large condensed structures, referred to as colloidal particles or large entities.

Because the assignments of peaks and the molecular description of these large colloidal species have not been established for  $R_m = 3$ , the investigation of this type of sols using NMR is difficult. In this case, we determined the fraction of the different species using the SAXS technique.

**B. SAXS.** *B1. Theory.* SAXS is produced by long and medium range (superatomic) heterogeneities in electron density of matter. If the sample is composed of identical and randomly oriented small particles (molecules, macromolecules, or colloidal species), immersed in a matrix of constant electronic density  $\rho_0$ , the scattered intensity  $I(q)$  is given by

$$I(q) = \phi P(q) S(q) \quad (1)$$

where  $\phi$  is the average number density of particles in the sample,  $P(q)$  is the orientation averaged form factor  $F(q)$  of the isolated particle:

$$P(q) = \langle |F(q)|^2 \rangle$$

and  $S(q)$  is the structure function which accounts for the interference between the wavelets scattered by each particle in the sample.

The form factor  $F(q)$  of a particle immersed in a matrix of average electronic density  $\rho_0$  depends on the spatial distribution electronic density  $\rho(r)$  inside the particle and is given by

$$F(q) = \int_{\text{volume of the particle}} [\rho(r) - \rho_0] \exp(i\vec{q} \cdot \vec{r}) d\vec{r}$$

In the simple case of spherical particles with radius  $R$ , volume  $V$ , and uniform density  $\rho$ ,  $P(q)$  is given by<sup>23</sup>:

$$P(q) = [V(\rho - \rho_0)]^2 \times \left[ 3 \frac{\sin(qR) - qR \cos(qR)}{(qR)^3} \right]^2 \quad (2)$$

For the factor  $V(\rho - \rho_0) = n$ ,  $n$  is the number of electrons in excess in the sphere volume,  $V$ , as compared to the number in an equivalent volume in the liquid matrix. The value  $P(0)$  is equal to  $n^2$  for spheres and also for particles of arbitrary shape even if the electron density  $\rho(r)$  is a varying function as in the case of small silicate species.

The structure function  $S(q)$  is the Fourier transform of the isotropic pair correlation function,  $g(r)$ .  $\phi g(r)$  represents the probability of finding a particle at a distance  $r$  from a particle situated at the origin. For an isotropic system:

$$S(q) = 1 + 4\pi\phi \int_0^\infty [g(r) - 1] \times r^2 \frac{\sin(qr)}{qr} dr$$

For spheres with no interactions other than impenetrability, the pair correlation function  $g(r)$  is zero for  $r < 2R$  and equal to 1 for  $r > 2R$ . Under these conditions  $S(q)$  is given by<sup>24,25</sup>

$$S(q) = 1 - 8F_v \left[ 3 \frac{\sin(2qR) - 2qR \cos(2qR)}{(2qR)^3} \right] \quad (3)$$

where  $F_v$  is the volume fraction ( $F_v = V/V_0$  and  $V_0 = 1/\phi$  = the average volume offered to each particle). For a "dilute"

**TABLE 3: Radii of Equivalent Spheres Calculated for Each Silicate Species**

oligomer	equivalent radius of a sphere (Å)
(1) monomer	3.06
(2) dimer	4.80
(3) linear trimer	6.54
(4) cyclic trimer	5.06
(5) linear tetramer	8.28
(6) cyclic tetramer	5.52
(7) branched cyclic trimer	6.54
(8) bridged cyclic tetramer	5.52
(9) monosubstituted cyclic tetramer	7.43
(10) bicyclic pentamer	6.30
(11) prismatic hexamer	5.71
(12) tricyclic hexamer	5.71
(13) cubic octamer	6.07
(14) tricyclic octamer	6.07
(15) tetracyclic nonamer	6.49

system of particles,  $S(q)$  is equal to 1 and then the scattered intensity (eq 1) is simply given by  $I(q) = \phi P(q)$ .

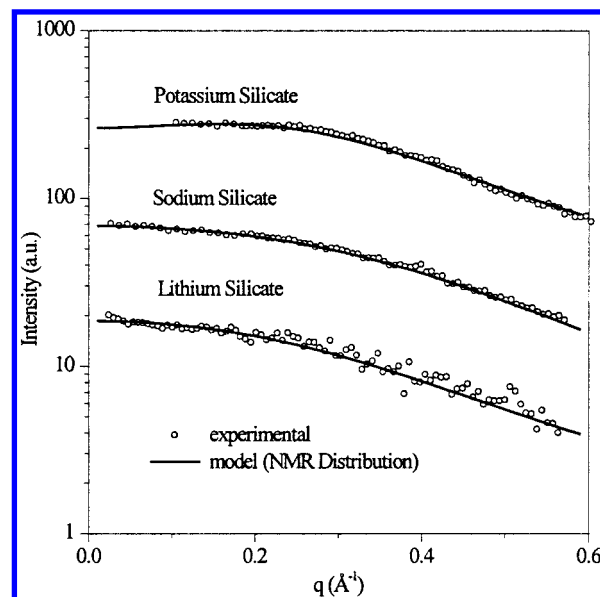
In the present study, we are facing to a rather complex system: the aqueous solution contains different types of particles (the silicate species) with a number of internal atomic arrangements and sizes. The observed SAXS is therefore produced by a set of very different and somewhat complex particles. In addition, interference effects in the scattering amplitude may occur.

**B2. Basic Assumptions.** To determine theoretically the SAXS intensity  $I(q)$  which is expected to be produced by the studied sols, which are composed of a set of different molecular species having a known structure, we have considered three simplifying assumptions: (i) SAXS intensity produced by the silicate species is assumed to be approximately the same as that produced by a set of spheres. This assumption is reasonable because, at very small  $q$ , SAXS intensity is insensitive to short-range variations in electron density and only depends on one geometrical parameter, the radius of gyration, or, in the case of spheres, on the radius of the particle. (ii) Weak interference effects observed in the scattering intensity are assumed to be predominantly due to particles of equivalent size. Even being a nonrigorous hypothesis, this approximation is expected to be acceptable for weak interference effects, and, in any case, it is a better approximation than simply considering a highly diluted set of particles. (iii) Because the contrast in electron density  $[\rho(r) - \rho_0]$  is an unknown varying function inside the different silicate species, the number of electrons in excess,  $n$  (eq 2), is simply assumed to be a constant, independent of the species nature. In the simple case of spherical particles with a constant electron density, this assumption is far from reality. Therefore, the assumption of an equivalent value of the excess in electron number,  $n$ , for all silicate species was considered a tentative hypothesis, which needs to be checked by applying it to a system in which the fractions of all molecular species are independently known.

The radius associated to each species was estimated from the known silicate structures identified by NMR as half the maximum diameter of the silicate network, without taking into account alkaline ions. Oxygen and silicon radii were taken equal to 1.32 and 0.42 Å,<sup>26</sup> respectively. The sphere radii assigned to every silicate species are listed in Table 3.

If the above-mentioned simplifying assumptions are applicable to the studied silicate solutions, the total scattered intensity can be determined as the sum of intensity contribution from each silicate species. Thus, we have

$$I_{\text{total}} = K \times \sum_i C_i \times P(q)_i \times S(q)_i \quad (4)$$



**Figure 5.** Experimental and simulation SAXS curves for silico-alkaline solutions for  $R_m = 2$ . Simulation curves were calculated using the species fraction determined from  $^{29}\text{Si}$  NMR experiments (see Table 2).

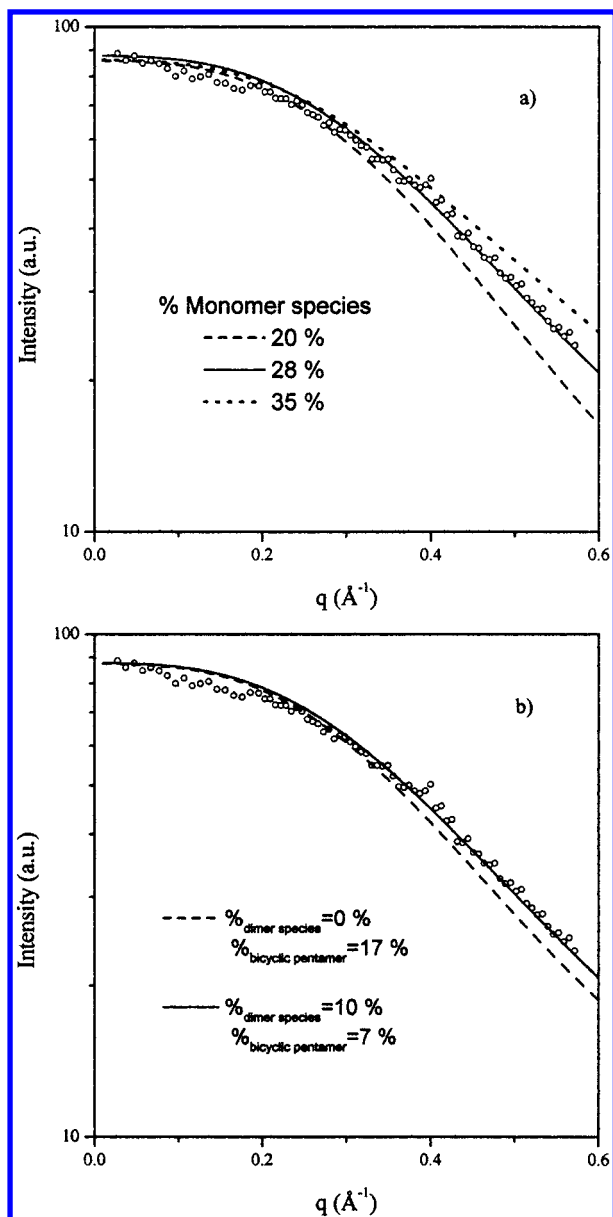
where  $C_i$ ,  $P(q)_i$ , and  $S(q)_i$  are the number fraction, averaged form factor, and structure function, respectively, of the different species.

**B3. Results Corresponding to Sols with a Silica/Alkaline Ratio  $R_m = 2$ .** The validity of the assumptions mentioned in the previous section was checked for silicate sols with  $R_m = 2$ . The theoretical intensity  $I(q)$  can be determined for these sols because the species fractions,  $C_i$ , are known from independent  $^{29}\text{Si}$  NMR measurements.

The  $P(q)$  functions corresponding to the different species were determined using eq 2 and the radius values listed in Table 3. A first calculation considering highly dilute solutions ( $F_v = 0$  or  $S(q) = 1$ ) lead to unacceptable fittings to the experimental curves. The theoretical functions  $I(q)$  were again calculated including the  $S(q)$  function given in eq 3. The only free parameters for the fittings were the volume fraction,  $F_v$ , and the ordinate scaling factor.

The experimental SAXS intensity curves and the theoretical functions corresponding to the best fitting of eq 4, for silico-alkaline solutions with a molar ratio  $R_m = 2$  containing  $\text{Li}^+$ ,  $\text{Na}^+$ , and  $\text{K}^+$  ions, are plotted in Figure 5. The good agreement between the theoretical and experimental intensity curves suggests that the simplifying assumptions for the determination of the SAXS intensity, described in the previous section, are reasonable and that the fraction of different silicate species,  $C_i$ , obtained by NMR (Table 2) are correct.

Rather small variations in the number fraction of any species produce significant deviations of the calculated curves from the experimental curves, as can be seen in Figure 6. In Figure 6a, the contribution of monomer species in scattering intensity appears clearly at high  $q$ . This contribution cannot be compensated by those of other species. For example, in Figure 6b, the fraction of dimers is added to the fraction of bicyclic species. The observed deviation illustrates the sensitivity of the procedure. On the other hand, this deviation cannot be compensated with a contribution of additional monomers because the resulting curve does not correspond to the experiment and the increase of the fraction's monomer from compensation should be too high compared to NMR data. The influence of large species will be illustrated in the following section for  $R_m = 3$ .

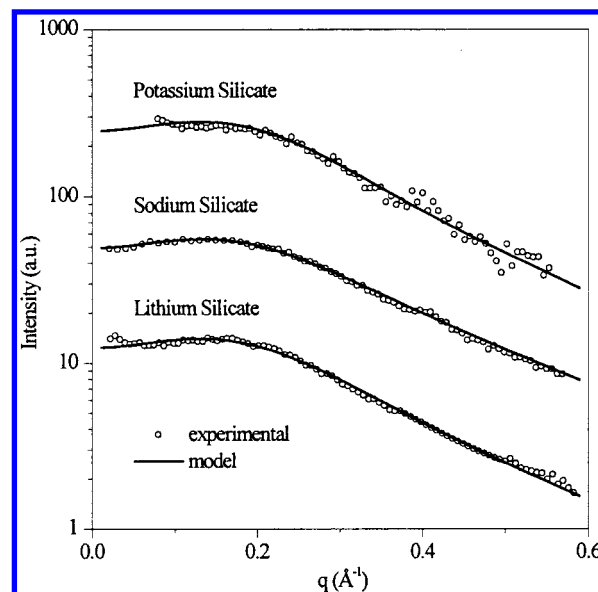


**Figure 6.** Experimental SAXS curve (○) for silica sols containing  $\text{Na}^+$  with  $R_m = 2$ : (a) three simulated curves considering different fraction of monomer species and (b) two simulated curves considering different fraction of dimers and bicyclic pentamers.

These results demonstrate that the SAXS procedure, even under the strong simplifying assumptions described, is adequate for quantitative determinations of the fractions of different silicate species in the studied sols.

**B4. Results Corresponding to Sols with  $R_m = 3$ .** As specified before, the number fractions of silicate species are not known from NMR measurements for solutions with a lower alkaline oxide content ( $R_m = 3$ ). Therefore, in this case we determined these fractions using SAXS data. The procedure was to vary the different species fractions until the best fitting of the theoretical intensity of eq 4 to the experimental functions was obtained. The experimental SAXS curves and those obtained with the respective fittings are plotted in Figure 7. The resulting fractions of silicate species,  $C_i$ , are listed in Table 4.

The radius of the large colloidal species has the same value, close to 10 Å, whatever the alkaline ions ( $\text{Li}^+$ ,  $\text{Na}^+$ , and  $\text{K}^+$ ). This seems to be true within about 10% because variations of 1 or 2 Å in the radius of the colloidal particles produce clearly unacceptable fittings, as can be seen in Figure 8b. The obtained



**Figure 7.** Experimental and simulation SAXS curves for silico-alkaline solutions for  $R_m = 3$ .

**TABLE 4: Distributions of Silicate Species in Number Percent Found from SAXS Experiments for Three Studied Silico-Alkaline Solutions with Silica/Alkaline Molar Ratios  $R_m = 3$**

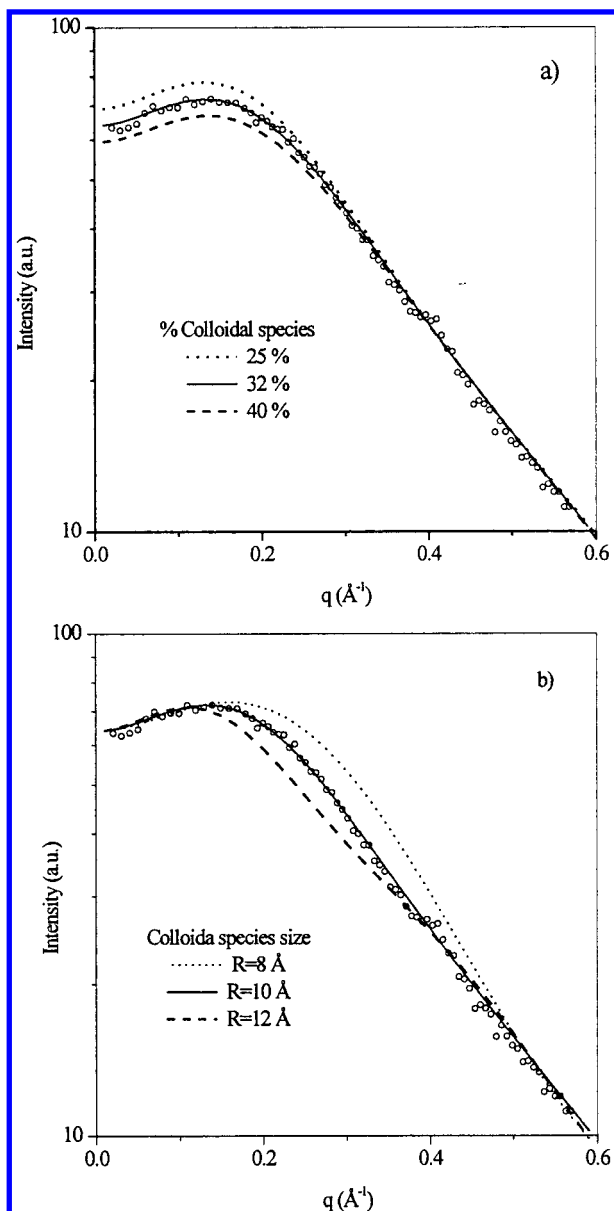
% oligomer	$R_m = 3$		
	$\text{SiO}_2\text{--Li}_2\text{O}$	$\text{SiO}_2\text{--Na}_2\text{O}$	$\text{SiO}_2\text{--K}_2\text{O}$
(1) monomer	8.0	10.0	6.0
(2) dimer	3.0	7.5	5.2
(3) linear trimer	0	7.2	0
(5) linear tetramer	3.8	5.4	8.0
(6) cyclic tetramer + (8) bridged cyclic tetramer	4.7	2.0	3.0
(7) branched cyclic trimer	0	2.9	0
(9) monosubstituted cyclic tetramer	10.5	1.9	6.8
(10) bicyclic pentamer	0	8.6	10.0
(11) prismatic hexamer + (12) tricyclic hexamer	9.0	10.0	11.2
(13) cubic octamer + (14) tricyclic octamer	2.2	2.1	2.8
(15) tetracyclic nonamer	11.0	10	10.9
colloidal species	47.8	32.4	36.1

fraction of these large species is a value estimated within 1%, as illustrated in Figure 8a.

Because the radius of the large colloidal species is equal to 10 Å, a number of structures may be assigned to the species. Some of the proposed structures for these species are shown in Figure 9. The large colloidal particles have several silicon nuclei with different environments, each of them giving a different contribution to  $^{29}\text{Si}$  NMR spectra.

To reduce the number of possible structures, the total amount of each structural unit  $Q^n$  ( $Q^1$ ,  $Q^2+Q^3$ ,  $Q^3$ ,  $Q^4$ ) was calculated by assuming both the distributions found previously (see Table 4) and the different proposed colloidal species (Figure 9). Table 5 gives the  $Q^n$  fractions calculated for each proposed structure. Each fraction corresponds to the contribution from all the silicon nuclei found in the same environment in all the silicate species.

The experimental data deduced from  $^{29}\text{Si}$  NMR (Figure 3) curves by integrating the peaks occurring in each  $Q^n$  region (see Table 1) and the calculated results are given in Table 5. The structures a and c were disregarded for all alkaline ions because their percentages were too far from experimental data. Conversely, the values corresponding to the structures f and g were close to the experimental data for all three types of silico-alkaline



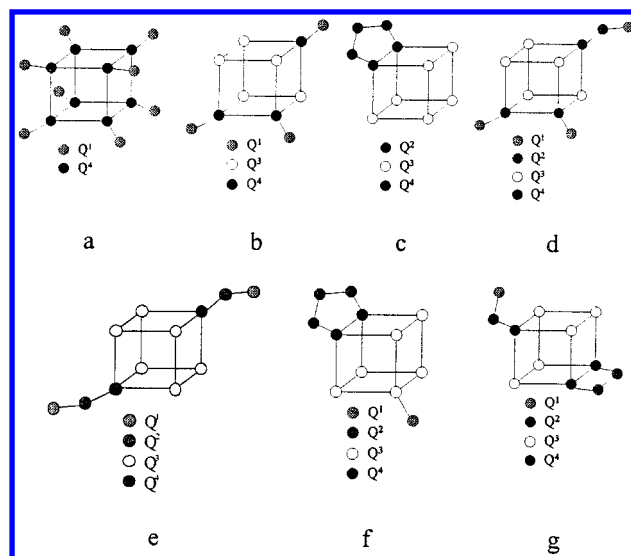
**Figure 8.** Experimental SAXS curve (○) for silica sols containing  $\text{Na}^+$  with  $R_m = 3$ : (a) three simulated curves considering different fraction of colloidal species and (b) three simulated curves considering different radii for the colloidal species.

solution (Table 5). The other structures (b, d, and e) cannot be disregarded as a probable structure for sodium solutions.

The individual fraction number of species determined from SAXS results for  $R_m = 3$  should be considered as a semiquantitative estimate, because different species may have a similar size and produce the same contribution to SAXS intensity, thereby impeding a unique conclusion. Nevertheless, the comparison between the results corresponding to  $R_m = 2$  and 3 allows one to establish qualitative and even semiquantitative conclusions about differences in the behavior and trends regarding the presence of small (monomers), medium, and large (cyclic molecule, colloidal particle) species.

#### IV. Discussion

To simplify the discussion, the fractions of silicate species given in Tables 2 and 4 were classified in five groups. One of them is composed only of monomers, a second one of linear species, the third of cycles molecules with 3 or 4 silicon nuclei, the fourth of cycles with 6 or 8 silicon nuclei, and the last of



**Figure 9.** Several possible structures for colloidal species with  $R = 10$  Å.

colloidal species. The simplified distributions obtained for  $R_m = 2$  and 3 are presented in Table 6 for each alkaline ion. It is apparent that, for molar ratio of 2, the major differences concern the group of linear species and cyclic entities with 6 or 8 Si groups. The fraction of linear species is a maximum for sodium and a minimum for lithium, whereas for cyclic group (6 or 8 Si), the opposite effect is observed. For potassium, the fractions are between those of sodium and lithium. For solutions with  $R_m = 3$ , the same evolution is observed on the linear and colloidal species. It is clearly seen that lithium enhances the formation of large species, i.e., cycles or colloidal particles, whereas sodium favors the formation of linear species.

It is known that pH strongly affects the distribution of silicate species in silico-alkaline solutions. To explain the differences observed on the distribution of silicate species for different alkaline ion and molar ratios, the pH of the studied solutions was measured. Results are presented in Table 7.

The increase in molar ratio ( $R_m 2 \rightarrow 3$ ) induces the decrease of pH in one unity independently of the alkaline ion. Therefore, the decrease in pH when  $R_m$  increases from 2 to 3 seems to enhance the formation of large species which is only observed for  $R_m = 3$ . At constant molar ratio (2 or 3), the pH of solution containing sodium silicate is higher than in lithium silicate solution. On the other hand, the pH remains approximately the same in sodium or potassium solutions.

If the only parameter affecting the distributions of silicate species is pH, the presence of maxima or minima in pH should be consistent with those corresponding to the species distribution. Our results indicate that differences in species distribution cannot be explained as an effect of pH only. In addition, the measure of pH of alkaline hydroxide solutions without silica, also presented in Table 7, show the same particularity concerning the lowest pH with solutions with lithium.

These conclusions indicate the existence of strong interactions between (i) alkaline ion and hydroxide and (ii) between alkaline ion and silicate species. Interaction (i) induces the differences associated with pH and suggests that interaction between lithium and hydroxide is stronger than interaction between sodium or potassium and hydroxide. Interaction (ii) is responsible for the differences in species distribution observed at a constant molar ratio and varying alkaline ion.

McCormick et al.<sup>14</sup> detected the presence of cation–anion pairs and demonstrated that the concentration of these pairs



**TABLE 5: Fraction (%) of Structural Units Q<sup>n</sup> Determined from Experimental Data and Those Calculated from Distributions Found from SAXS Experiments Using Several Assumptions for the Structure of the Colloidal Species (the Corresponding Structures Are Shown in Figure 8)**

% Q <sup>n</sup>	R <sub>m</sub> = 3											
	SiO <sub>2</sub> –Li <sub>2</sub> O				SiO <sub>2</sub> –Na <sub>2</sub> O				SiO <sub>2</sub> –K <sub>2</sub> O			
	Q <sup>1</sup>	Q <sup>2</sup> + Q <sup>3Δ</sup>	Q <sup>3</sup>	Q <sup>4</sup>	Q <sup>1</sup>	Q <sup>2</sup> + Q <sup>3Δ</sup>	Q <sup>3</sup>	Q <sup>4</sup>	Q <sup>1</sup>	Q <sup>2</sup> + Q <sup>3Δ</sup>	Q <sup>3</sup>	Q <sup>4</sup>
exp	6.9	26.7	42.6	19.9	15.1	33.8	38.6	4.2	8.3	27.0	37.5	19.0
a	39.2	10.8	12.3	36.9	34.4	19.5	15.0	30.5	37.9	15.4	12.4	33.1
b	21.0	14.0	45.9	18.0	18.9	24.1	42.0	14.1	21.7	19.4	41.8	15.6
c	3.0	32.0	51.9	12.0	4.8	38.2	46.7	9.4	6.1	35.1	47.0	10.4
d	19.8	18.9	43.3	17.0	18.1	27.5	40.1	13.5	20.6	23.4	39.7	14.9
e	14.2	24.6	49.0	11.3	13.6	32.0	44.6	9.0	15.7	18.4	24.8	19.7
f and g	8.5	30.2	43.3	17.0	9.1	36.5	40.1	13.5	10.7	33.3	39.7	14.9

**TABLE 6: Simplified Distributions of Silicate Species for Two Sets of Three Sols with Silica/Alkaline Molar Ratios of 2 and 3**

% oligomer	SiO <sub>2</sub> /Li <sub>2</sub> O		SiO <sub>2</sub> /Na <sub>2</sub> O		SiO <sub>2</sub> /K <sub>2</sub> O	
	2	3	2	3	2	3
monomer (1)	34.2	8.0	28.3	10.0	33.7	6.0
linear (2), (3), and (5)	19.5	6.8	29.3	20.1	22.1	13.2
cycle to 3 or 4 Si (4) and (6–10)	23.5	15.2	29.8	15.4	31	19.8
cycle to 6 or 8 (11–15)	22.8	22.2	12.6	22.1	13.2	24.9
colloidal species	0	47.8	0	32.4	0	36.1

**TABLE 7: pH of Silico-Alkaline Solutions and Alkaline Hydroxide Solutions**

SiO <sub>2</sub> (mol·L <sup>-1</sup> )	A <sub>2</sub> O (mol·L <sup>-1</sup> )	R <sub>m</sub>	pH, A = Li	pH, A = Na	pH, A = K
1.5	0.75	2	11.8	12.5	12.7
	0.5	3	11.1	11.5	11.6
0	0.75		13.1	13.7	13.6
	0.5		13.2	13.9	13.8

increases with increasing cation size. These authors also concluded that large alkali-metal cations combine chemically more easily with large silicate oligomers because of their larger polarizability. A stronger polarizability would enhance the interaction of the alkalines with the larger charge volume of big oligomers (cyclic molecules or colloidal species). The conclusions of McCormick et al.<sup>14</sup> are confirmed by our results concerning the solutions containing sodium or potassium, as listed in Table 6.

An apparent disagreement was observed for solutions containing lithium, which have a fraction of large particles higher than those containing sodium or potassium (Table 6). However, it is well known<sup>27</sup> that the size of lithium ion including its sphere of hydration is larger than sodium or potassium ions and may be as large as rubidium ion. Thus, the enhancing action of lithium on the formation of large species is consistent with the general conclusion of McCormick et al.<sup>14</sup>

## V. Conclusion

<sup>29</sup>Si NMR spectroscopy and SAXS have consistently described the distribution of the different silicate species in the silico-alkaline solutions and allowed us to establish the relative influence of each alkaline ion on the fraction of the different species.

Using a model elaborated from <sup>29</sup>Si NMR data, the determination of distributions of silicate species from SAXS data was demonstrated to be possible and appears to be reasonably precise. This novel procedure may eventually be applied to other similar solutions.

On the other hand, the coupling of NMR and SAXS allowed us to describe the structure of the large colloidal species existing in the studied sols. An interesting result was that the size of these species is identical ( $R = 10$  Å) regardless of the base.

Therefore, the type of alkaline ion affects the fraction of the species but does not appreciably change their structure.

Further studies will be carried out to determine the influence of alkaline ion content on the second stage of the ASR, i.e., during the destabilization of silico-alkaline solutions by addition of calcium leading to silico-calco-alkaline gels.

## References and Notes

- (1) Stanton, T. E. *Trans. Amer. Soc. Civ. Engrs.* **1942**, 107, 54.
- (2) Gajda, J. *World Cement Res. Dev.* **1996**, 58.
- (3) Dent Glasser, L. S.; Kataoka, N. *Cement Concr. Res.* **1981**, 11, 1.
- (4) Hansen, W. C. *J. Am. Concr. Inst.* **1944**, 40, 213.
- (5) Dron, R.; Brivot, F. *Cement Concr. Res.* **1992**, 22, 941.
- (6) Chatterji, S.; Thaulow, N.; Jensen, A. D. *Cement Concr. Res.* **1989**, 19, 177.
- (7) Wen, Z. Formation et caractérisation de sols alcalins de silice. Conditions de leur transformation en gel au contact de sels et d'hydroxydes, notamment de ceux qui sont présents dans le béton. Etude particulière du rôle de la portlandite. Ph.D. Thesis, Université de Bourgogne, 1989.
- (8) Michaud, V. Simulation expérimentale de l'alcali-réaction des bétons. Etude de l'influence des ions sulfate. Ph.D. Thesis, Université de Bourgogne, 1995.
- (9) Gaboriaud, F.; Chaumont, D.; Nonat, A.; Hanquet, B.; Craievich, A. *J. Sol-Gel Sci. Technol.* **1998**, 13, 353.
- (10) Iler, R. K. *The Chemistry of Silica*; John Wiley & Sons: New York, 1979.
- (11) Dent Glasser, L. S.; Lachowski, E. E.; Cameron, G. G. *J. Appl. Chem. Biotechnol.* **1977**, 27, 39.
- (12) Dent Glasser, L. S. *Chem. Br.* **1982**, 33.
- (13) Harris, R.; Bahlmann, K. F.; Metcalfe, K.; Smith, E. G. *Magn. Reson. Chem.* **1993**, 31, 743.
- (14) McCormick, A. V.; Bell, A. T.; Radke, C. J. *J. Phys. Chem.* **1989**, 93, 1733.
- (15) Michaud, V.; Nonat, A.; Sorrentino, D. Experimental simulation of mechanisms involved in the building of stresses in concretes subjected to alkali-silica reaction.; *Proceedings of the 10th International Congress on the Chemistry of Cement*; Justnes, H., Ed.; Gothenburg, Norway, 1997; 4iv049.
- (16) Nieto, P.; Dron, R.; Thevenot, R.; Zanni, H.; Brivot, F. *C. R. Acad. Sci. Paris* **1995**, t. 320, 485.
- (17) Iler, R. K. Colloidal Components in Solutions of Sodium Silicate. In *Soluble Silicates*; Falcone, Ed.; American Chemical Society: Washington, DC, 1982; pp 95.
- (18) Andersson, K. R.; Glasser, L. S.; Smith, D. N. Polymerization and Colloid Formation in Silicate Solutions. In *Soluble Silicates*; Falcone, Ed.; American Chemical Society: Washington, DC, 1982; pp 115.
- (19) Harris, R. K.; Newman, R. H. *J. Chem. Soc. Faraday Trans.* **1977**, 2, 1204.
- (20) Harris, R. K.; Knight, C. T. G. *J. Chem. Soc., Faraday Trans.* **1983**, 2, 1525.
- (21) Engelhardt, G.; Michel, D. *Height-Resolution Solid-State NMR of Silicates and Zeolites*; John Wiley & Sons: New York, 1987.
- (22) McCormick, A. V.; Bell, A. T.; Radke, C. J. *Stud. Surf. Sci. Catal.* **1986**, 28, 247.
- (23) Rayleigh, L. *Proc. R. Soc.* **1911**, A-84, 25.
- (24) Debye, P. *Phys. Z.* **1927**, 28, 135.
- (25) Guinier, A. *X-Ray Diffraction in Crystals, Imperfect Crystals, and Amorphous Bodies*; Dover Publications, Inc.: New York, 1994.
- (26) *Handbook of Chemistry and Physics*; Weast, R. C., Ed.; CRC Press: Cleveland, 1977.
- (27) Brinker, C. J.; Scherer, G. W. *Sol-Gel Science: The Physics and Chemistry of Sol-Gel Processing*; Academic Press: New York, 1990.